Bioorganic & Medicinal Chemistry 18 (2010) 8512–8529

Contents lists available at ScienceDirect

Bioorganic & Medicinal Chemistry

journal homepage: www.elsevier.com/locate/bmc

High-throughput identification of antibacterials against methicillin-resistant *Staphylococcus aureus* (MRSA) and the transglycosylase

Ting-Jen Rachel Cheng, Ying-Ta Wu, Shih-Ting Yang, Kien-Hock Lo, Shao-Kang Chen, Yin-Hsuan Chen, Wen-I Huang, Chih-Hung Yuan, Chih-Wei Guo, Lin-Ya Huang, Kuo-Ting Chen, Hao-Wei Shih, Yih-Shyun E. Cheng, Wei-Chieh Cheng, Chi-Huey Wong *

Genomics Research Center, Academia Sinica, 128 Sec 2 Academia Road, Nankang, Taipei 115, Taiwan

ARTICLE INFO

Article history:
Received 20 August 2010
Revised 11 October 2010
Accepted 14 October 2010
Available online 21 October 2010

Keywords:
Transglycosylase
High-throughput screening
Methicillin-resistant *Staphylococcus aureus* (MRSA)
Salicylanilide

ABSTRACT

To identify new transglycosylase inhibitors with potent anti-methicillin-resistant *Staphylococcus aureus* (MRSA) activities, a high-throughput screening against *Staphylococcus aureus* was conducted to look for antibacterial cores in our 2 M compound library that consists of natural products, proprietary collection, and synthetic molecules. About 3600 hits were identified from the primary screening and the subsequent confirmation resulted in a total of 252 compounds in 84 clusters which showed anti-MRSA activities with MIC values as low as 0.1 μg/ml. Subsequent screening targeting bacterial transglycosylase identified a salicylanilide-based core that inhibited the lipid II polymerization and the moenomycin-binding activities of transglycosylase. Among the collected analogues, potent inhibitors with the IC_{50} values below 10 μM against transglycosylase were identified. The non-carbonhydrate scaffold reported in this study suggests a new direction for development of bacterial transglycosylase inhibitors.

© 2010 Elsevier Ltd. All rights reserved.

1. Introduction

With the widespread emergence of methicillin- and vancomycin-resistant bacterial infections, there are increasing interests in the search of new targets for antibiotics discovery and development. Most of antibiotics currently in use can be classified as the following classes: (1) β-lactam and glycopeptide antibiotics targeting cell wall biosynthesis;[1] (2) aminoglycoside, tetracycline and macrolide antibiotics targeting protein synthesis;[2,3] (3) fluoroquinolones targeting DNA gyrase and topoisomerase.[4] To tackle the problem of drug resistance, one can focus on these proven targets and develop new drugs to overcome drug-induced resistance that is caused by mutations of the targets or modifications of the antibiotics. Another strategy is to identify new targets for discovery of new classes of antibiotics.

Bacterial cell wall, also called peptidoglycan, consists of repeating β-1,4-linked *N*-acetylglucosaminyl-*N*-acetylmuramyl units cross-linked through peptide side chains. The biosynthesis of peptidoglycan has been the target for several classes of antibiotics, yet most of these antibiotics target the peptide cross-linking step by inhibiting the enzyme transpeptidase directly (e.g., β-lactam antibiotics), or by forming a complex with the last two residues D-ala-D-ala dipeptides (e.g., vancomycin).[5] In fact, peptidoglycan biosynthesis consists of several stages (Fig. 1).[6,7] First, UDP-*N*-acetylglucosamine (GlcNAc) is converted to UDP-*N*-acetylmuramyl (MurNAc)-pentapeptide in the cytoplasm through the actions of MurA-F. The muramyl pentapepide was then transferred from UDP to a bactoprenol C55 lipid chain and then the unit was moved to the membrane interface to form lipid I. Lipid I was then linked to GlcNAc through MurG-catalyzed reactions to form lipid II which is then flipped across the membrane to its outer face. Finally, lipid II was polymerized by linking the disaccharide pentapeptide to the 4-OH group of GlcNAc of the existing peptidoglycan strand by transglycosylation, followed by cross-linking of the peptide chain by transpeptidation. The step prior to the transpeptidation in the peptidoglycan biosynthesis is catalyzed by a single protein moiety, penicillin-binding protein (PBP) or bi-functional transglycosylases (TGase).[8] It occurs at the outer face of the membrane and therefore should be an appealing target for antibiotic discovery. Though β-lactam antibiotics, which interrupt the transpeptidation step,[9] have been used clinically in the past 60 years, no antibiotics have been developed to target TGase except moenomycin A (**1**, Fig. 2), which has only been used in animals.[10–13]

In the past years, significant efforts have been directed toward development of new antibacterial agents to target TGase, but with slow progress.[14–16] We decided to conduct a high-throughput screening of a collection of 2 million compounds in our library

Abbreviation: TGase, transglycosylase; SA, *Staphylococcus aureus*; MRSA, methicillin-resistant *Staphylococcus aureus*.

* Corresponding author. Tel.: +886 2 27899400; fax: +886 2 27853852.
E-mail address: chwong@gate.sinica.edu.tw (C.-H. Wong).

0968-0896/$ - see front matter © 2010 Elsevier Ltd. All rights reserved.
doi:10.1016/j.bmc.2010.10.036

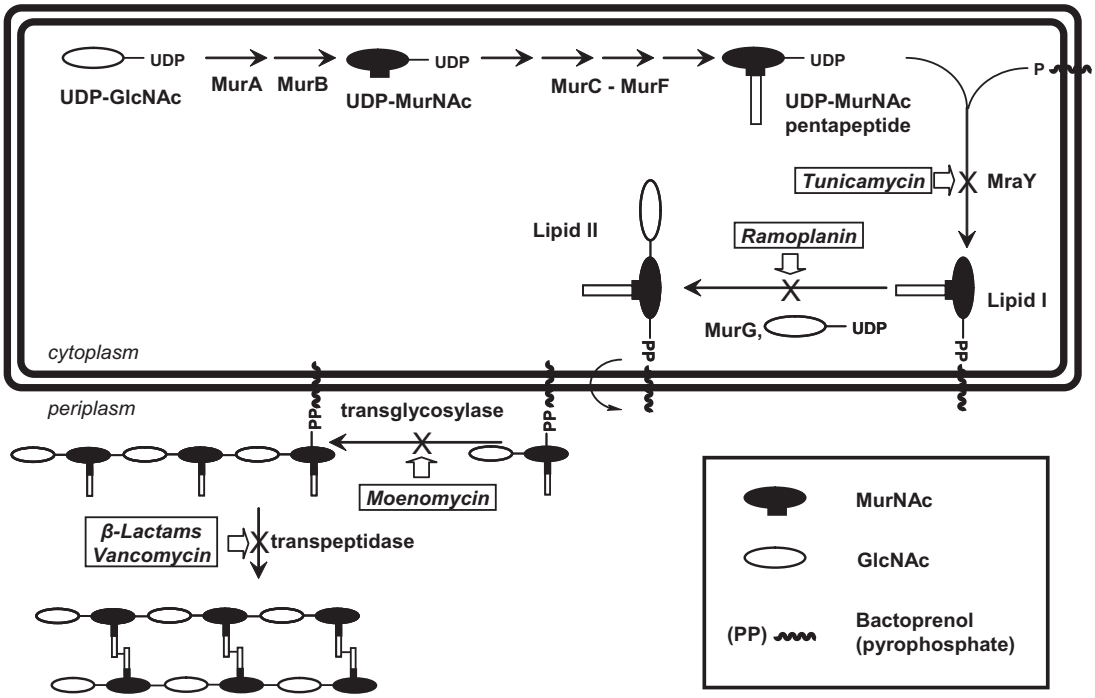

Figure 1. Bacterial cell wall biosynthesis.[7]

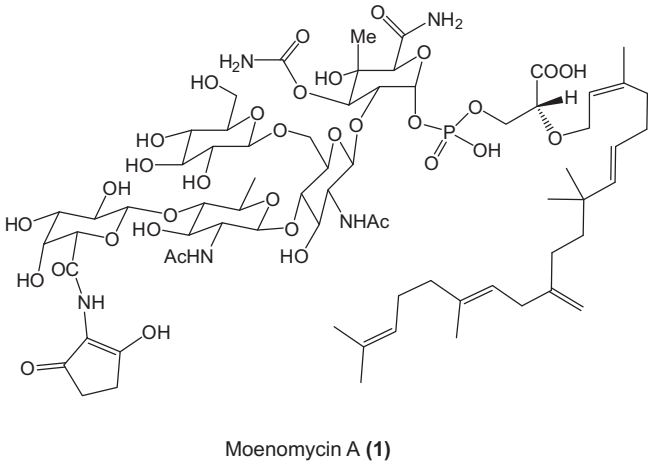

Figure 2. Structure of moenomycin A (**1**).

by using the GNF HTS system capable of screening nearly one million molecules a day for identification of new hits against wild-type *Staphylococcus aureus* (SA). The confirmed hits were then tested for activities against methicillin-resistant *Staphylococcus aureus* (MRSA) and for TGase inhibition. This strategy led to the identification of new anti-MRSA agents and non-carbohydrate compounds which showed TGase inhibition activities.

2. Results and discussion

2.1. HTS campaign of antibacterial agents

We aim to identify potent anti-MRSA molecules that targets bacterial TGase. Therefore, our strategy was to employ HTS for identification of hits against SA and subsequently screen the hits for anti-MRSA and inhibiting TGase activities (Fig. 3). We did not screen the 2 M compound library for anti-MRSA activities directly because MRSA is highly pathogenic and the HTS system has to be operated in an open space. An assay protocol for screening of anti-SA compounds in 1536-well plates was thus established. A log-phase culture of SA at 0.1 OD_{600}/ml was diluted in various folds and 5 μl of the diluted culture was dispensed into the wells of the plates for growing for overnight. After addition of Alamar blue, the obtained signals and the coefficient variance (CV) were compared. The result showed that the optimal dilution fold of culture for screening was between 2000 and 8000 that is, 20–75 cells/well of a 1536-well plate (Fig. 4A). The best coefficient of variation using this protocol is below 5%. *Z′* value[17] and signal to background ratio was determined as 0.7 and 20, respectively. This HTS assay was also used to determine the MIC values of known antibiotics against wt SA to validate the assay. A plate with 8-point threefold serial dilutions of antibiotics was thus prepared and assayed using the same protocol as described above. The MIC_{90} values determined using this assay are comparable to the values determined using the traditional micro-dilution method in 96-well plates (data not shown).

For the HTS campaign, plates that contain antibiotics in serial dilutions were tested every 50 plates to ensure the screening quality and validity. In the primary screening, a remaining activity of less than 0.6 (inhibition of bacterial growth by 60%) was used as the threshold for hits, which were initially clustered into 175 groups (Fig. 4B). About 3600 compounds were selected for determination of the MIC values against wild-type SA as well as MRSA and evaluation of TGase inhibition (Fig. 3).

2.2. Profiling of the antibacterial activities of the identified hits

The primary hits were further narrowed down to 252 compounds in 84 clusters that showed the MIC values, ranging from 0.03 μg/ml to 8 μg/ml against wild-type SA as well as several MRSA strains (Fig. 5 and Tables 1–8). Not surprisingly, known antibiotics were identified in the screen and represent unique clusters. For example, cluster 2 is fluorouracil and cluster 8 contains fluorodeoxyuridines, cluster 9 is vancomycin, cluster 10 is mitomycin,

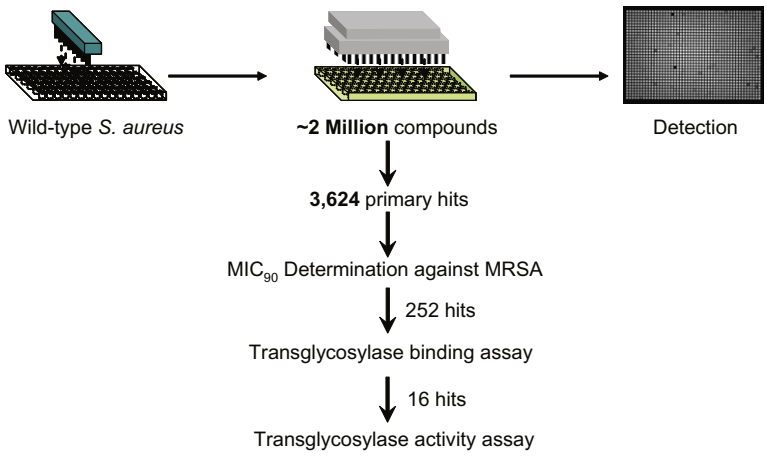

Figure 3. The flow chart of identification of TGase inhibitors from 2 M library.

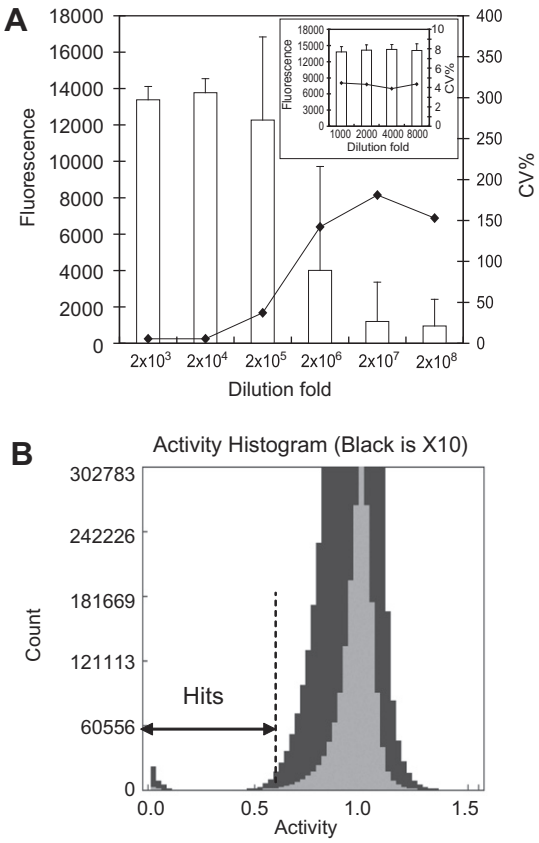

Figure 4. High-throughput assay development and validation of antibacterial screening in 1536-well plates. (A) The fluorescence intensity and the coefficient of variation (CV) values versus bacteria culture in various dilutions. Bacterial growth in 1536-well plates. Various dilutions of SA culture at 0.1 OD_{600}/ml were dispensed into the wells of a 1536-well plate, incubated for 20 h and the cell growth was monitored using 20% Alamar blue. The image and fluorescence intensities were taken with Viewlux. (B) HTS campaign of antibacterial screens. The remaining activity after inhibition of each individual compound was counted and accumulated for the decision of hits. In this activity histogram, a remaining activity less than 0.6 was used as the threshold to obtain the primary screening hits.

cluster 25 is novobiocin, cluster 29 is narasin, cluster 41 contains actinomycins, and cluster 45 is moenomycin. As show in Figure 5B, several privileged antibacterial scaffolds such as naphthalamides in cluster 17, nitrofurans in cluster 49 and 77, sulfonamides in cluster 38 indeed were identified from our libraries.

Some of clusters enabled preliminary structure activity relationship. For example, cluster 7 (Table 1) was a 2-acylamino-1,3,4-oxadiazole-based library. When an electron withdrawing group such as a fluoro or trifluoromethyl group was at the *para* or *meta* position (R^1 or R^2), the compounds 7-1 to 7-12 showed strong antibacterial activity (MIC <3 μg/ml) against all test strains. In contrast, when the substituent was a methyl, or *tert*-butyl group, the compounds such as 7-18, 7-19, and 7-20 were all inactive (see Supplementary data). The cluster 33 was a pyrimidine-based library. When the substituent R^3 was an aryl group, compounds 33-1 to 33-8 (except 33-7) showed strong antibacterial activity (Table 4). However, if the substituent R^3 changed to an alkyl group, the compounds such as 33-9 and 33-10 became inactive (see Supplementary data).

The hits were further tested for their activities against other bacteria (Table 9). Most of these hits, except some salicylanilides and nitrofuranyls, have little activities against Gram-negative bacteria such as *Acinetobacter baumannii*, *Escherichia coli*, and *Pseudomonas aeruginosa*.

2.3. Bacterial transglycosylase inhibitors

The anti-MRSA hits were further evaluated for transglycosylation inhibition using the fluorescence anisotropy (FA) assay for competing the binding of moenomycin A (**1**, Fig. 2) to TGase,[18] followed by confirmation based on TGase-catalyzed lipid II polymerization.[16] Among 252 compounds tested, 16 molecules at 100 μM inhibited at least 90% of the binding between TGase and moenomycin (Table 10). Further tests on TGase-catalyzed lipid II polymerization revealed that only 42-10 (**2**, Fig. 6A) showed complete inhibition of enzymatic activities of TGase. A close analogue 42-17 (Table 10) inhibited up to 90% of TGase activities while another compound 42-2 hardly inhibited the lipid II polymerization.

We further collected salicylanilide analogues (42-21 to 42-54) from commercial sources and screened them for lipid II polymerization inhibition activities. It was interesting to note that salicylanilides that contain only two aromatic rings, that is, 42-1 to 42-9 in Table 6 hardly inhibited lipid II polymerization activities when compounds were tested at 100 μM. Most salicylanilides bearing an extra hydrophobic group(s), such as an aryl group in ring B showed complete inhibition activities when tested at 100 μM (Tables 11 and 12). Overall, compounds 42-30 (**3**), 42-31 (**4**), and 42-35 (**5**) (Fig. 6A, Table 12) were the most active TGase inhibitors identified in the series. Analysis of the screening data showed that salicylanilides containing two rings (scaffold I, Fig. 6B) showed no TGase inhibition activities. An additional hydrophobic group(s) to

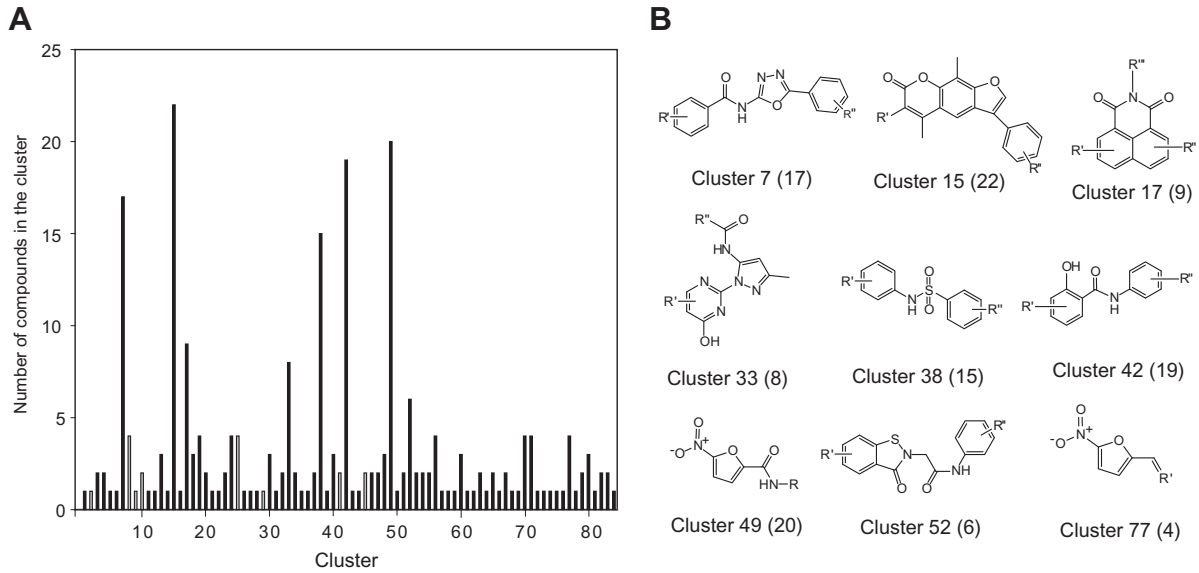

Figure 5. Active hits against MRSA. (A) The confirmed hits consisted of 84 clusters. Gray bars represent known antibiotics while black bars are for molecules from compound library. (B) Representative clusters of the confirmed hits.

Table 1
Anti-SA and -MRSA activities of compounds in the cluster 7

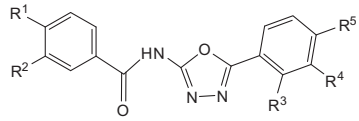

Compd	R^1	R^2	R^3	R^4	R^5	MIC (μg/ml)			
						SA	MRSA1	MRSA2	MRSA3
7-1	H	CF_3	Cl	H	H	1	0.5	2	0.5
7-2	H	Cl	H	H	F	1	0.5	1	4
7-3	H	Br	H	H	F	2	0.5	1	1
7-4	H	CF_3	H	H	F	0.5	0.5	1	4
7-5/7-12[a]	H	CF_3	H	H	Cl	1	0.5	0.125	0.125
7-6	H	F	H	H	Br	2	0.5	0.5	0.5
7-7	H	CF_3	H	H	Br	1	1	0.5	0.125
7-8	H	Cl	H	H	Cl	0.5	0.25	0.125	0.125
7-9	H	Br	H	H	Cl	0.5	0.5	2	2
7-10	F	H	H	Br	H	3	1.5	1.5	1.5
7-11	CF_3	H	H	H	Cl	3	1.5	1.5	1.5
7-13	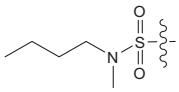	H	H	$-OCH_3$	H	4[b]	8[b]	16[b]	32[b]

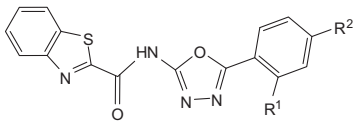

Compd	R^1	R^2	MIC (μg/ml)			
			SA	MRSA1	MRSA2	MRSA3
7-14	Cl	H	2	2	2	32
7-15	CH_3	CH_3	0.5	0.5	0.25	0.25
7-16	$-S-CH_3$	H	4	2	2	4
7-17	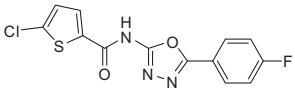		1.2[b]	1.2[b]	1.2[b]	1.2[b]

[a] These two compounds have different registry codes in our library and therefore were treated as two independent compounds.
[b] The MIC in μg/ml was calculated from the MIC determined in μM.

Table 2
Anti-SA and -MRSA activities of compounds in the cluster 15

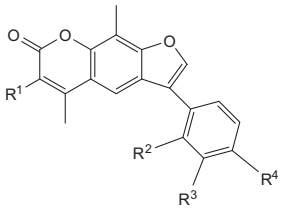

Compd	R^1	R^2	R^3	R^4	MIC (μg/ml)			
					SA	MRSA1	MRSA2	MRSA3
15-1		H	H	Br	2	2	16	2
15-2	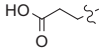	H	H	CH_3	1	2	1	2
15-3		H	H	Br	0.5	1	0.5	1
15-4	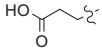	H	H	Cl	2.5	1.25	2.5	2.5
15-5	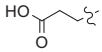	H	OCH_3	H	2.5	2.5	2.5	2.5
15-6		H	H	CH_3	5	2.5	2.5	2.5
15-7	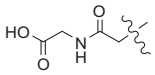	H	H	Cl	1.25	1.25	1.25	1.25
15-8	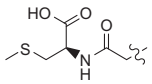	H	H	Cl	2.5	1.25	2.5	2.5
15-9	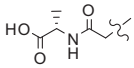	H	H	Cl	0.3	1.25	0.3	1.25
15-10	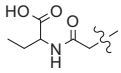	H	H	Cl	2.5	5	2.5	2.5
15-11	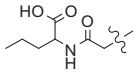	H	H	Cl	1.25	2.5	2.5	1.25
15-12	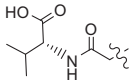	H	H	Cl	1.25	1.25	2.5	2.5
15-13	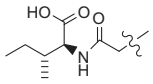	H	H	Cl	2.5	2.5	2.5	2.5
15-14	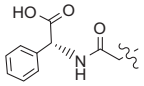	H	H	Cl	2.5	2.5	2.5	2.5
15-15	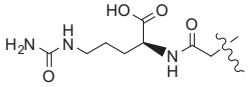	H	H	Cl	1.25	2.5	2.5	2.5
15-16	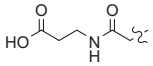	H	H	Cl	2.5	1.25	2.5	2.5
15-17	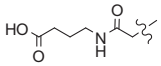	H	H	Cl	2.5	2.5	2.5	2.5
15-18	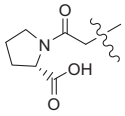	H	H	Cl	0.3	0.3	0.3	0.6
15-19	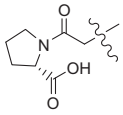	H	H	F	0.6	1.25	0.6	0.6

Table 2 (*continued*)

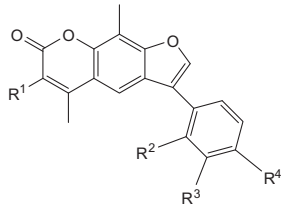

Compd	R^1	R^2	R^3	R^4	MIC (μg/ml)			
					SA	MRSA1	MRSA2	MRSA3
15-20	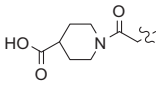	H	H	F	2.5	1.25	2.5	2.5
15-21	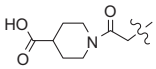	H	H	Cl	2.5	1.25	2.5	2.5
15-22	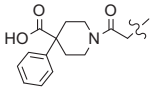	H	H	Cl	2.5	2.5	2.5	2.5

Table 3
Anti-SA and -MRSA activities of compounds in the cluster 17

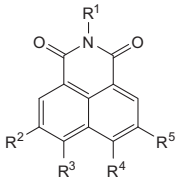

Compd	R^1	R^2	R^3	R^4	R^5	MIC (μg/ml)			
						SA	MRSA1	MRSA2	MRSA3
17-1		H	NO_2	NO_2	H	2.5	2.5	1.25	1.25
17-2		H	NO_2	NO_2	H	5	2.5	2.5	2.5
17-3		NO_2	H	H	NO_2	1.25	2.5	0.125	0.125
17-4	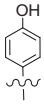	NO_2	H	H	NO_2	2.5	2.5	2.5	0.3
17-5		NO_2	H	H	NO_2	1.25	2.5	2.5	0.3
17-6	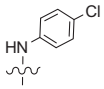	NO_2	H	H	NO_2	2.5	2.5	2.5	2.5
17-7		H	H	NO_2	H	8	2	8	8
17-8	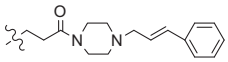	H	H	H	H	0.5	1	4	0.25
17-9	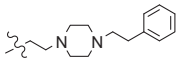	H	H	H	H	1	1	16	0.5

Table 4
Anti-SA and -MRSA activities of compounds in the cluster 33

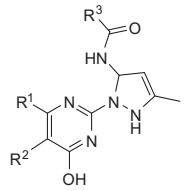

Compd	R^1	R^2	R^3	MIC (μg/ml)			
				SA	MRSA1	MRSA2	MRSA3
33-1	C_2H_5	H		1	4	2	1
33-2	C_2H_5	H		1.2[a]	1.2[a]	1.2[a]	1.2[a]
33-3	C_3H_7	H		2	8	8	8
33-4	C_3H_7	H		2	0.5	1	1
33-5	C_3H_7	H		1	0.5	1	2
33-6	C_3H_7	H		1	1	1	1
33-7	CH_3	CH_3	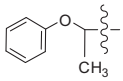	1	0.25	1	1
33-8	CH_3	C_2H_5		0.5	1	0.5	0.5

[a] The MIC in μg/ml was calculated from the MIC determined in μM.

Table 5
Anti-SA and -MRSA activities of compounds in the cluster 38

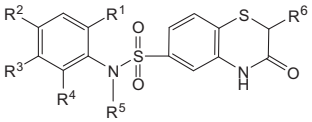

Compd	R^1	R^2	R^3	R^4	R^5	R^6	MIC (μg/ml)			
							SA	MRSA1	MRSA2	MRSA3
38-1	CH_3	H	H	H	H	CH_3	1.2[a]	1.2[a]	1.2[a]	1.2[a]
38-2	H	H	CH_3	CH_3	H	CH_3	2	64	16	16
38-3	CH_3	CH_3	H	H	H	CH_3	2	32	4	>64
38-4	C_2H_5	H	H	H	H	CH_3	0.5	1	32	1
38-5	CH_3	CH_3	H	H	H	C_2H_5	1	8	4	>64
38-6	CH_3	H	Cl	H	H	C_2H_5	4	>64	16	16
38-7	CH_3	CH_3	H	CH_3	H	C_2H_5	2	64	32	>64
38-8	OC_2H_5	H	H	H	CH_3	CH_3	4	8	8	>64

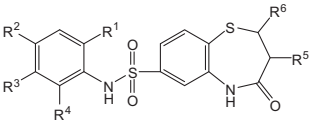

38-9	C_2H_5	H	H	H	H	CH_3	2	8	4	>64
38-10	CH_3	CH_3	H	H	CH_3	H	2	2	16	>64
38-11	C_2H_5	H	H	H	CH_3	H	2	2	4	>64
38-12	CH_3	H	CH_3	H	CH_3	H	2	16	32	>64
38-13	Br	CH_3	H	H	CH_3	H	2	8	16	>64

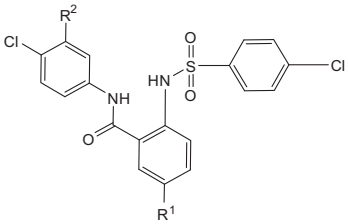

Compd	R^1	R^2	MIC (μg/ml)			
			SA	MRSA1	MRSA2	MRSA3
38-14	Br	H	0.25	0.25	0.25	0.5
38-15	Cl	Cl	0.25	0.25	0.25	0.25

[a] The MIC in μg/ml was calculated from the MIC determined in μM.

the two-ring salicylanilides (scaffold II, Fig. 6B) would result in inhibition of lipid II polymerization activities.

Computer-aided modeling of compound **2** in complex with TGase revealed five potential binding sites after blind docking (Fig. 7A). Among the five potential sites, the one received the highest score (~32%; avg score = −9 kcal/mol) was the hydrophobic pocket where TGase binds to moenomycin.[19] In complex with the recently determined *E. coli* (EC) TGase,[19] the binding model (Fig. 7B) predicted that three potential hydrogen-bond interactions were found between the A-ring hydroxyl group and Glu323, between the linker amide nitrogen atom and the Asn275 side chain, and between the ether oxygen and the backbone nitrogen of Tyr315. In addition, it was predicted that ring A of **2** may form a potential cation-pi interaction with Arg325 or pi–pi interaction with Tyr315, which could strengthen the affinity of **2** to TGase. The ring C of **2** may interact with the hydrophobic pocket formed by Lys274, Tyr310, Ile314, Val354, and Ala357 (Fig. 7B).

Based on the modeling analysis, several compounds were synthesized to identify the essential moieties in compound 42-10 (**2**) for TGase inhibition activities (Fig. 7C). It was experimentally confirmed that the hydroxyl moiety at the 2 position in ring A plays an important role for TGase inhibition, as deletion (**6**, Fig. 7C) or methylation of the hydroxyl group (**7**, Fig. 7C) resulted in a loss of TGase inhibition activity. When the amide moiety in **2** was changed to the imine and amine moiety to generate compound **8** and **9** (Fig. 7C), respectively, no TGase inhibition activity was observed, indicating the amide group really affects the enzyme inhibition. In addition, when we introduced an ester group in ring C, the compound **10** showed the moderate inhibition against TGase (IC_{90} = 50 μM). In contrast, compound **11** bearing an extra carboxylic acid in ring C was inactive at 100 μM after hydrolysis of **10** in basic conditions.

The K_i and IC_{50} values of the four selected compounds (**2**–**5**) against TGase from EC, SA, and *M. tuberculosis* (Mtb) were further compared using FA-based assay and lipid II polymerization analysis, respectively (Table 13). Compound **5** showed the lowest K_i and IC_{50} values towards EC TGase. Unfortunately, FA-binding analysis cannot be applied to TGase from SA nor TGase from Mtb due to low signal-to-noise ratios. In terms of inhibition on enzymatic activities, it was surprisingly found out that compounds **2–5** can inhibit the enzymatic activities of SA TGase, but not the activities of Mtb TGase. In theory, compounds **2**–**5** could compete moenomycin binding from EC TGase, implying that they shall bind to the conserved region for all TGases. As illustrated in Figure 8, although the binding site of **2** looks similar, a couple of key residues (compared to Asn141, Asp145, and Trp187 of the reference structure MtgA with PDB code 3hzs[20]) are different among species, which may cause the variation of binding affinity of the compound for TGase. The interactions with the hydrophobic pocket (e.g., formed by Lys140, Tyr176, Ile180, Val223, and Pro226 in the reference structure 3hzs shown in Fig. 8A) were mostly conserved; however, the hydrogen-bond interactions with the ring A hydroxyl group and with linker amide nitrogen were different. In the case of EC TGase (PDB code 3fwl[19]), resembled interactions were kept by

Table 6
Anti-SA and -MRSA activities of compounds in the cluster 42.

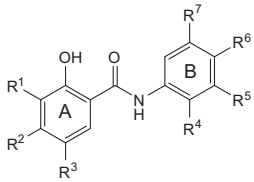

Compd	R^1	R^2	R^3	R^4	R^5	R^6	R^7	MIC (μg/ml)			
								SA	MRSA1	MRSA2	MRSA3
42-1	Br	H	Br	H	Cl	Cl	Cl	⩽0.03	0.06	⩽0.03	⩽0.03
42-2/42-9[a]	Cl	H	Cl	H	Cl	Cl	H	0.25	1	1	1
42-3	Cl	H	Cl	H	Cl	Cl	Cl	0.125	0.5	1	0.125
42-4	Br	H	Br	H	H	Cl	H	1	4	1	1
42-5	Br	H	Br	Cl	H	H	Cl	1	1	0.5	0.5
42-6	Cl	H	Cl	Cl	H	H	Cl	1	0.5	0.5	2
42-7	Cl	H	Cl	H	Cl	Cl	Cl	0.5	0.5	1	1
42-8	Br	H	Br	H	H	H	Cl	2	2	2	8
42-10	Br	H	Br	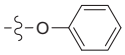	H	H	Cl	0.5	0.25	0.5	0.5
42-11	Br	H	Br	Cl	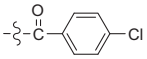	H	Cl	0.5	2	8	8
42-12	Br	H	Br	Cl	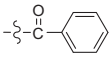	H	Cl	1	8	4	4
42-13	Br	H	Cl	Cl	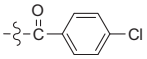	H	Cl	0.5	0.5	1	0.5
42-14	Br	H	Br	Cl	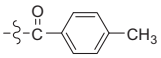	H	Cl	>4	>4	>4	>4
42-15	H	H	Cl	H	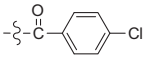	Cl	H	>4[b]	>4[b]	>4[b]	>4[b]
42-16	Br	H	Br	H	H	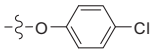	Cl	0.5	0.25	0.25	0.5
42-17	Br	H	Cl	Cl	H	Cl	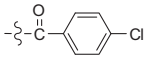	0.25	0.25	0.25	0.25
42-18	Br	H	Br	H	H	Cl	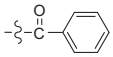	1	1	2	1
42-19	Br	H	Cl	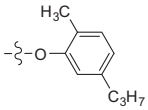	H	H	Cl	0.25	0.125	0.06	0.06

[a] These two compounds have different registry codes in our library and therefore were treated as two independent compounds.
[b] The MIC in μg/ml was calculated from the MIC determined in μM.

Glu323 and Asn275, respectively. In addition, a cation–pi interaction between Arg325 and the ring A of **2** could be exerted (Fig. 7B). On the other hand, SA TGase (PDB code 2olv[21]) can only form hydrogen bonds via Asp156 and Gln161 (Fig. 8B). The Mtb TGase (structure model),[22] however, does not have the aforementioned hydrogen bonds and cation–pi interactions when **2** binds to the same site (Fig. 8C).

It was also noticed that salicylanilides have MIC values of 1–10 μM for SA and IC_{50} values for SA TGase inhibition ranging 10–40 μM (Table 13). Since TGase is on the outer surface of bacteria, it is unlikely that the permeability to cell membrane is a factor for the difference. It is, however, possible that salicylanilides have other bacterial targets to exert its overall antibacterial activities. In fact, salicylanilides with the structures as scaffold I, but not scaffold II (Fig. 6B), have been reported to have a wide range of pharmacological activities, such as anti-bacterial,[23] anti-tubucular,[24] anti-inflammatory[25] and anti-cancer[26] activities. Depending on the substituents attached to the anilide group of salicylanilides, salicylanilides have been reported to interact with differential targets. For example, analogues with alkylcarbamates or N-protected amino acid esters on the phenyl group were reported to target Mycobacterium species[24,27] or 14-3-3 zeta protein.[25] On the other hand, salicylanilides containing the 2,3-hydroxy-benzanilide structural motif would inhibit autophosphorylation of the KinA kinase in bacteria for survival.[28] In this report, we identified that salicylanilides with an aryl moiety on the aniline moiety (Scaffold II in Fig. 6B) showed inhibitor activities towards bacterial TGase.

It was interesting that addition of a third ring was shown to reduce antibacterial activities yet enhanced its potency in TGase inhibition. Whether addition and optimization of a third ring would increase the affinity of small molecules towards TGase and less to other targets remained to be investigated.

3. Conclusion

In this study, we conducted high-throughput campaign for TGase inhibitors that shows potent anti-MRSA activities. A total of 252 compounds in 84 clusters, including known antibiotics, were identified as potent anti-MRSA hits. Salicylanilide-based molecules were further confirmed to have TGase inhibition activities.

After evaluating the inhibition activities of various salicylanilide analogues, it was concluded that an extra aryl group to the anilide

Table 7
Anti-SA and -MRSA activities of compounds in the cluster 49

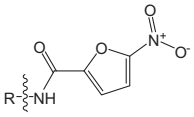

Compd	R	MIC (μg/ml)			
		SA	MRSA1	MRSA2	MRSA3
49-1	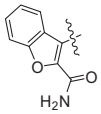	2	0.5	0.5	2
49-2	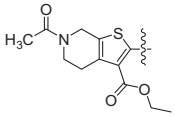	1	4	1	1
49-3	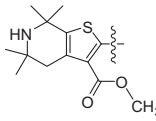	2	2	4	2
49-4		2	0.25	0.25	0.25
49-5		2	0.5	0.5	0.5
49-6	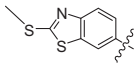	1	1	1	1
49-7		4	1	2	2
49-8	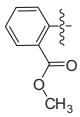	8	0.5	4	2
49-9	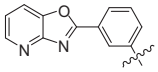	4	4	2	2
49-10	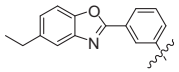	1	0.5	1	4
49-11	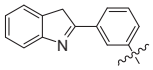	0.5	0.25	0.5	0.5
49-12/49-20[a]	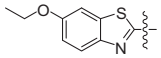	2	4	16	16
49-13		2	2	2	2
49-14	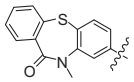	2	1	0.5	2
49-15	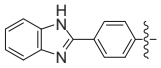	0.125	0.25	8	4
49-16	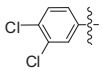	2	2	4	>4
49-17	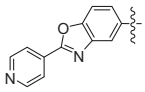	2	4	2	>4

Table 7 (*continued*)

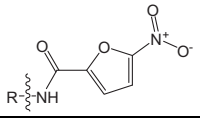

Compd	R	MIC (μg/ml)			
		SA	MRSA1	MRSA2	MRSA3
49-18	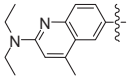	2	>4	>4	>4
49-19	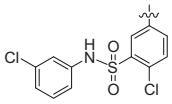	1.5	1.5	1.5	1.5

[a] These two compounds have different registry codes in our library and therefore were treated as two independent compounds.

Table 8
Anti-SA and -MRSA activities of compounds in the cluster 77

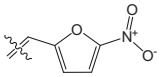

Compd	MIC (μg/ml)			
	SA	MRSA1	MRSA2	MRSA3
77-1 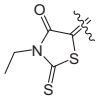	0.5	0.5	0.125	0.25
77-2	0.25	1	2	1
77-3 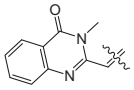	1	2	1	0.5
77-4 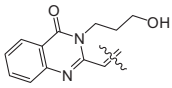	2	2	2	2

was essential for TGase inhibition activities. The molecules (scaffold II in Fig. 6B) showed selective inhibition to TGase from EC and SA, but not TGase from Mtb.

As the only TGase inhibitor moenomycin is a complex type of glycolipid and difficult to synthesize,[29,30] the non-carbohydrate scaffold discovered in this study provides a new direction to the development of TGase inhibitors as new antibiotics.

4. Experimental

4.1. Materials

Wild-type *Staphylococcus aureus* (ATCC 29213), MRSA (MRSA1, ATCC 33592), *Bacillus subtilis* (ATCC 23587), *Actinetobacter baumannii* (ATCC 49139), *Escherichia coli* (ATCC 25923), *Haemophilus influenzae* (ATCC 49247), *Proteus mirabilis* (ATCC 25933), *Pseudomonas aeruginosa* (ATCC 25619), *Serratia marcescens* (ATCC 14756), *Stenotrophomonas maltophilia* (ATCC 13637) were obtained from American Type Culture Collection (ATCC). *Mycobacterium smegmatis* (BCRC11565) were obtained from Bioresource Collection and Research Center in Taiwan. NTUH4722 (MRSA2) is a clinical isolate

resistant to oxacillin, ampicllin, gentamicin, clindamycin, minocycline, sulfamethoxazole and trimethoprim, and was kindly provided by Dr. Po-Ren Hsueh at National Taiwan University Hospital (Taipei, Taiwan). Sa-OXA-R2 (MRSA3) is a clinical isolate resistant to oxacillin and was kindly provided by National Health Research Institute in Taiwan (Miaoli, Taiwan).

4.2. Compound libraries

All compounds were solubilized in 100% DMSO at 10 mM in 96-well plates. Subsequently, the compounds were diluted to 1 mM and dispensed into 1536-well plates (for HTS) or 384-well plates (for hit-picking). The compound plates were stored at −50 °C until use. Our library is composed of ~1.8 M commercial small molecules, ~5000 known inhibitors and approved drugs, ~60,000 pure natural products, and ~70,000 proprietary collections. The library can be clustered into about 5300 groups, based on 85% structure similarity, and the diversity is about 0.87 calculated by a modified centroid-diversity sorting algorithm.[31]

4.3. Chemoinformatics and screening data analysis

Chemoinformatics were applied mostly at two stages to assist HTS, namely compound management in the primary screening stage and decision-making in the post screening stage. An in-house system was established with application tools for compound inventory and registration. The diversity of the library was calculated by a modified centroid-diversity sorting algorithm.[31] A web-based graphical user interface (GUI) was designed for viewing individual assay plate for online quality control and signal histogram for the decision of screening hits. In the post screening data analysis, structural clustering method, based on the Scitegic FCFP_4 descriptors (Pipeline Pilot, Accelrys Inc., San Diego) and Tanimoto similarity distance between hits,[32] was applied to check the overall screening quality and outliers which were need of further validation. Hit compounds with Tanimoto factor of 0.85 were clustered together and member size of each cluster family was recorded.

4.4. High-throughput screening

Screens were performed in 1536-well plates at the Genomics Research Center of Academia Sinica in Taiwan using the high-throughput screening (HTS) system manufactured by GNF systems (GNF, San Diego, CA). The HTS system is integrated with dispensers, a 1536-pin transferring tool, incubators and a ViewLux plate reader (Perkin Elmer Inc.). For screening, wild-type SA (ATCC 29213) at 0.1 $O.D._{600}$ in Muller-Hinton broth were diluted in 1:2000 and the diluted culture were dispensed into 1536-well plates at 5 μl/well (75 cells/well) followed by compound transfer using a 1536-pin transferring device with 50-nl slots (V&P Scientific, San Diego, CA, USA). After covered with GNF-designed lids to minimize edge effects from evaporation, the plates were incubated in the environmentally controlled incubators (37 °C, 80% humidity) for 20 h. After incubation, 20% Alamar blue (Biosource, San Diego, CA) was added at 5 μl/well with the reagent dispenser, and incubated for 1 h. The fluorescence was monitored with the Viewlux reader at 595 nm wavelength. The interested primary hits were picked with a hit-picking system manufactured by GNF systems, which is integrated with a dispenser (Tecan). The compound identities were further confirmed with LC–MS (Bruker). The compounds that showed correct mass and >90% purity were used for confirmation analysis using the same protocol described above.

4.5. Determination of minimal inhibition concentration (MIC)

The minimal inhibitory concentration of tested compounds was determined following the NCCLS standard. The experiments were conducted in 384-well microtiter plates using 8-point twofold dilutions in Muller-Hilton broth. Exponentially growing cells at 5×10^5 cells/ml were incubated with test compounds at various concentrations in a final volume of 50 μl. After an 18 h to 24 h incubation at 37 °C, 20% Alamar blue were dispensed into the wells of the plates and the fluorescence was measured with a plate reader (EnVision, Perkin Elmer). The minimal concentration of the compound that prevents at least 90% bacterial growth was determined as the MIC_{90} value of a given molecule.

4.6. Fluorescence anisotropy-based transglycosylase assay

The identified anti-SA hits were cherry-picked in wells of a 1536 plate. Bifunctional TGases (i.e., full-length PBP) from EC, SA, and Mtb were incubated at 10 μg/ml with 100 nM fluorescent moenomycin in 10 mM Tris, 100 mM NaCl, pH 8.0 at a final volume of 10 μl in wells of 1536-well plates (Stand-Alone dispenser, GNF system, San Diego, CA, USA).[18] One microliter of 1 mM compound stocks were added to wells using an automated liquid handling system (Bravo, Agilent Automation System-Velocity 11). The last two columns of every plate were 10 μM moenomycin and 2.5% DMSO used as positive and negative controls, respectively. After a 30-min incubation, decreases in fluorescence anisotropy, which was caused by compound binding to TGase and fluorescent probe was released, were determined with Viewlux. Hits that showed greater than 90% reduction compared to the control anisotropy values were selected for lipid II polymerization assay. For determination of the binding affinity of a given compound, various

Table 9
Profiling of antibacterial activities of compounds in some clusters

Bacteria	#	MIC (μg/ml) of compounds in the cluster							
		7	15	17	33	38	42	49	77
Gram-Positive									
S. aureus	ATCC29213	0.5–2	0.5–2	0.5–4	1–8	0.5–2	⩽0.03–8	1–4	0.25–4
MRSA1	ATCC33593	0.5–2	1–2	1–64	1–8	0.5–4	⩽0.03–8	2–16	0.5–4
MRSA2	NTUH4722	0.5–2	0.5–16	4–64	1–8	0.5–4	⩽0.03–8	4–32	0.125–4
MRSA3	Sau-Oxa-R2	2–32	1–2	0.25–64	1–32	0.5–4	⩽0.03–8	4–32	0.25–4
B. subtilis	ATCC23857	0.5–2	>64	4–64	0.25–1	<0.03–4	⩽0.03–8	0.06–1	<0.03–0.13
Gram-Negative									
E. coli	ATCC29213	>256	>256	>256	>256	>256	8 to >256	256	16 to >256
P. aeruginosa	ATCC25619	>256	>256	>256	>256	>256	16 to >256	128	2 to >256
A. baumannii	ATCC49139	>256	>256	>256	>256	>256	16 to >256	12 to >256	>256
S. maltophilia	ATCC13637	>256	>256	>256	>256	>256	16 to >256	32 to >256	>256
S. marscescens	ATCC14756	>256	>256	>256	>256	>256	16 to >256	32 to >256	>256
M. smegatis	BCRC11565	0.5–8	1 to >64	4 to >64	0.25–2	>64	0.5–8	0.5 to >64	1 to >64

Table 10
Lipid II polymerization inhibition activities of the compounds that showed greater than 90% inhibition in moenomycin binding

Compd	Structure	Inhibition %[a]		Compd	Structure	Inhibition %[a]	
		Binding[b] (%)	Activity[c] (%)			Binding[b] (%)	Activity[c] (%)
13-2	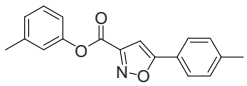	96	0	42-2	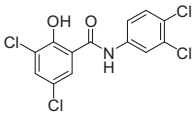	90	0
13-3	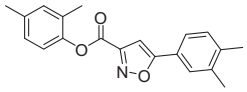	95	0	42-10 (**2**)	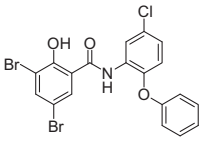	97	100
14-1	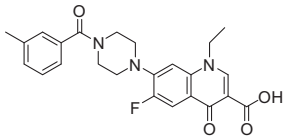	93	0	42-17	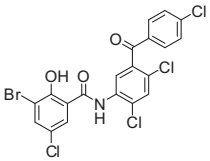	92	90
15-4	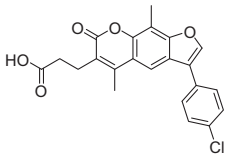	97	0	49-13	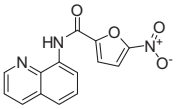	90	0
15-5	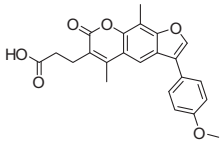	90	0	49-14	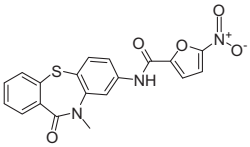	91	0
31-1	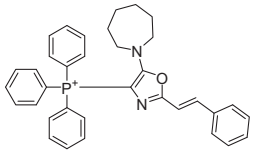	97	0	49-16	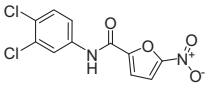	96	0
37-1	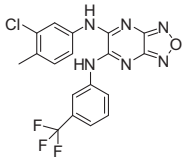	90	0	49-18	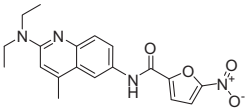	90	0
40-2	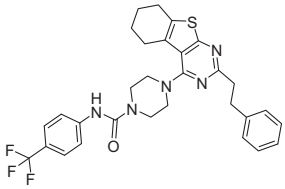	90	0	70-1	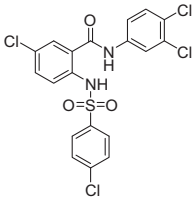	98	0

[a] Inhibition percentage was determined at 100 μM of compound.
[b] Binding inhibition was evaluated using the fluorescence anisotropy assay using fluorescein-labeled moenomycin as the probe.[18]
[c] Activity inhibition was evaluated using the polymerization of fluorescent lipid II as described in Section 4. The percentage was calculated using the percentage of the peak area of the substrate.

concentrations of the compound were incubated with TGase and fluorescent moenomycin for 30 min and the polarization values was measured as described above. The K_i values were derived from K_d and IC_{50}.[33]

4.7. Lipid II polymerization assay

Fluorescent lipid II was prepared using chemoenzymatic synthesis of lipid II followed by labeling lipid II with a fluorescent probe and a HPLC-based analysis for lipid II polymerization was conducted as reported (Fig. 9).[16] Briefly, *Micrococcus flavus* vesicles (6.4 mg) were incubated with 100 mM UDP-MurNAc, 200 mM UDP-GlcNAc, 10 mg undecaprenyl monophosphate in buffer (50 mM Tris–HCl, pH 8, 10 mM $MgCl_2$, and 1% (w/v) Triton X-100) with a final volume of 100 μL for 20 min.[34] After purification by normal phase chromatography followed by reverse phase HPLC, lipid II was added with a solution of nitrobenzoxadiazole (NBD)[35] and was stirred at room temperature for overnight. The mixture was concentrated, redissolved in 1:1 v/v water/methanol and purified by semi-preparative chromatography on a Zorbax RX-C8 column (9.4 mm × 250 mm, 5 μm particle size). TGase assays were carried out by incubating 100 μM nitrobenzoxadiazole

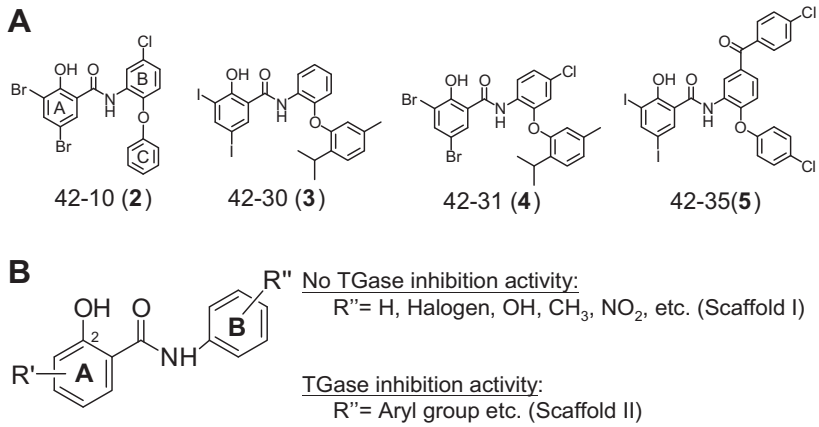

Figure 6. Compounds that showed potent inhibition activities against bacterial TGase. (A) Inhibitors identified in this study. (B) Salicylanilides can be grouped into two scaffolds. Molecules with scaffold I showed no TGase inhibition activities whereas molecules with scaffold II can inhibit TGase activities.

Table 11
TGase inhibition activities and antibacterial activities of salicylanilides that contains an aromatic ring attached to ring B via a carbonyl bond

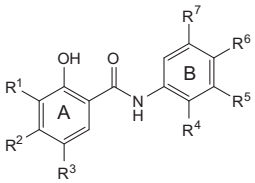

Compd	R^1	R^2	R^3	R^4	R^5	R^6	R^7	IC_{90} of TG inhibition activity	MIC (μg/ml)	
									SA	MRSA1
42-11	Br	H	Br	Cl	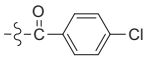	H	Cl	100 μM	0.5	2
42-12	Br	H	Br	Cl	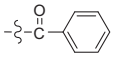	H	Cl	100 μM	1	8
42-13	Br	H	Cl	Cl	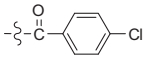	H	Cl	100 μM	0.5	0.5
42-14/42-27[a]	Br	H	Br	Cl	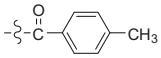	H	Cl	100 μM	>4	>4
42-17	Br	H	Cl	Cl	H	Cl	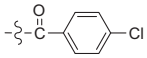	100 μM	0.25	0.25
42-18	Br	H	Br	H	H	Cl	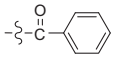	100 μM	1	1
42-21	I	H	I	H	H	Cl	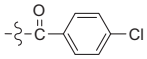	100 μM	⩽2	4
42-22	I	H	I	H	H	Cl	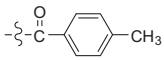	100 μM	4	4
42-23	H	H	Cl	Cl	H	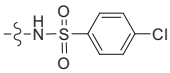	H	>100 μM	16	32
42-24	I	H	I	Cl	H	H	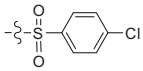	100 μM	8	8
42-25	H	H	Cl	H	H	Cl	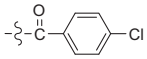	100 μM	4	4
42-26	Br	H	Br	H	Cl	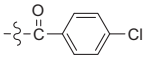	H	100 μM	⩽2	4
42-28	Br	H	Br	H	H	Br	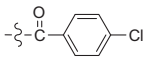	100 μM	⩽2	⩽2
42-29	Br	H	Br	Cl	H	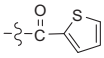	H	>100 μM	4	4

[a] These two compounds have different registry codes in our library and therefore were treated as two independent compounds.

Table 12
TGase inhibition activities and antibacterial activities of salicylanilides that contains an aromatic ring attached to ring B via an ether bond

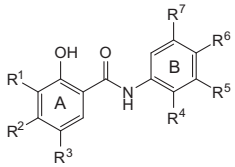

Compd	R^1	R^2	R^3	R^4	R^5	R^6	R^7	IC_{90} of TG inhibition activity	MIC (μg/ml)	
									SA	MRSA1
42-10 (**2**)	Br	H	Br	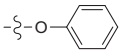	H	H	Cl	50 μM	0.5	0.25
42-16	Br	H	Br	H	H	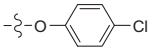	Cl	100 μM	0.5	0.25
42-30 (**3**)/42-38[a]	I	H	I	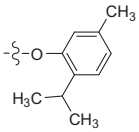	H	H	H	⩽25 μM	4	2
42-31 (**4**)	Br	H	Br	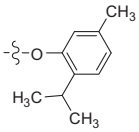	H	Cl	H	⩽25 μM	1	1
42-32	Br	H	Br	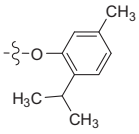	H	H	H	50 μM	1	4
42-33	H	H	Cl	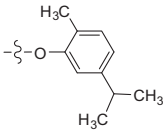	H	H	Cl	100 μM	0.5	0.5
42-34	Br	H	Cl	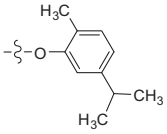	H	H	Cl	50 μM	1	0.5
42-35 (**5**)	I	H	I	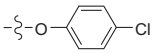	H	H	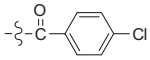	⩽25 μM	8	4
42-36	I	H	I	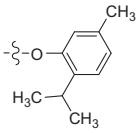	H	H	Cl	50 μM	4	0.5
42-37	Cl	H	Cl	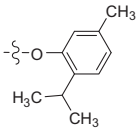	H	H	Cl	50 μM	1	0.25
42-39	I	H	Cl	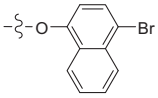	H	H	Cl	100 μM	8	4
42-40	Br	H	Br	H	H	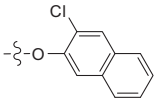	Cl	100 μM	4	4
42-41	Br	H	Cl	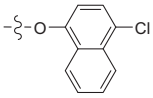	H	H	Cl	100 μM	8	16
42-42	I	H	Cl	H	H	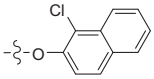	Cl	>100 μM	4	⩽2

Table 12 (*continued*)

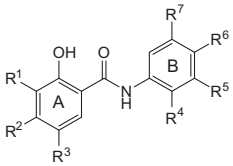

Compd	R^1	R^2	R^3	R^4	R^5	R^6	R^7	IC_{90} of TG inhibition activity	MIC (μg/ml)	
									SA	MRSA1
42-43	I	H	I	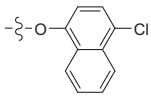	H	H	Cl	50 μM	4	⩽2
42-44	Br	H	Br	H	H	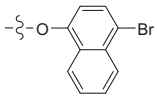	Cl	100 μM	4	⩽2
42-45	Cl	H	Cl	H	H	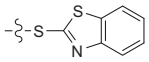	Cl	>100 μM	8	4
42-46	Cl	H	Cl	H	H	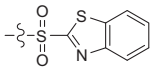	Cl	100 μM	8	4
42-47	Br	H	Br	H	H	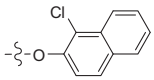	Cl	100 μM	⩽2	⩽2
42-48	I	H	I	H	H	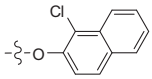	Cl	>100 μM	8	8
42-49	Br	H	Cl	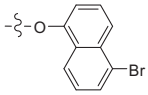	H	H	Cl	100 μM	4	⩽2
42-50	Br	H	Cl	H	H	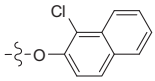	Cl	100 μM	⩽2	⩽2
42-51	Br	H	Br	H	H	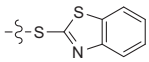	Cl	100 μM	4	⩽2
42-52	Br	H	Br	H	H	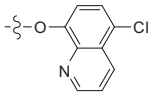	Br	50 μM	32	16
42-53	Br	H	Br	H	H	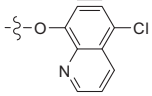	Cl	100 μM	16	32
42-54	Br	H	Br	H	H	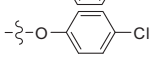	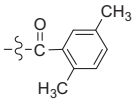	>100 μM	8	32

[a] These two compounds have different registry codes in our library and therefore were treated as two independent compounds.

Table 13
MIC, K_i and IC_{50} of compounds against various bacteria and its TGase, respectively

	MIC_{90} (μM)/K_i of TGase binding (μM)[a]/IC_{50} of TGase activity (μM)[b]					
	EC	SA[c]	MRSA1[c]	MRSA2[c]	MRSA3[c]	*Mycobacterium* spp.[d]
Moenomycin A (**1**)	160/1.1/0.028	3/ND[e]/0.034	11/ND[e]/0.034	33/ND[e]/0.034	33/ND[e]/0.034	2.5/9.8/0.05
42-10 (**2**)	>512/98/30.3	1/ND[e]/37.5	0.5/ND[e]/37.5	1/ND[e]/37.5	1/ND[e]/37.5	0.5/ND[e]/NI[f]
42-30 (**3**)	>512/98/7.2	6.5/ND[e]/27.8	3.3/ND[e]/27.8	1.6/ND[e]/27.8	13/ND[e]/27.8	13/ND[e]/NI[f]
42-31 (**4**)	>512/NI/2.7	1.8/ND[e]/19.6	1.8/ND[e]/19.6	1.8/ND[e]/19.6	0.45/ND[e]/19.6	3.6/ND[e]/NI[f]
42-35 (**5**)	>512/68/2.1	11/ND[e]/9.3	5.5/ND[e]/9.3	11/ND[e]/9.3	11/ND[e]/9.3	44/ND[e]/NI[f]

[a] K_i was calculated using the K_d value determined using fluorescence anisotropy binding assay.[18,33]
[b] IC_{50} was determined using TGase-catalyzed lipid II polymerization.
[c] TGase from SA, MRSA1, MRSA2, and MRSA3 are the same.
[d] For mycobacterium species, MIC was determined with *Mycobacterium smegatis* and TG inhibition evaluation was done with TGase from *M. tuberculosis*.
[e] ND: Can not be determined due to low signal-to-noise ratio.
[f] NI: The compound showed no inhibition activities for TGase from *M. tuberculosis* at 100 μM.

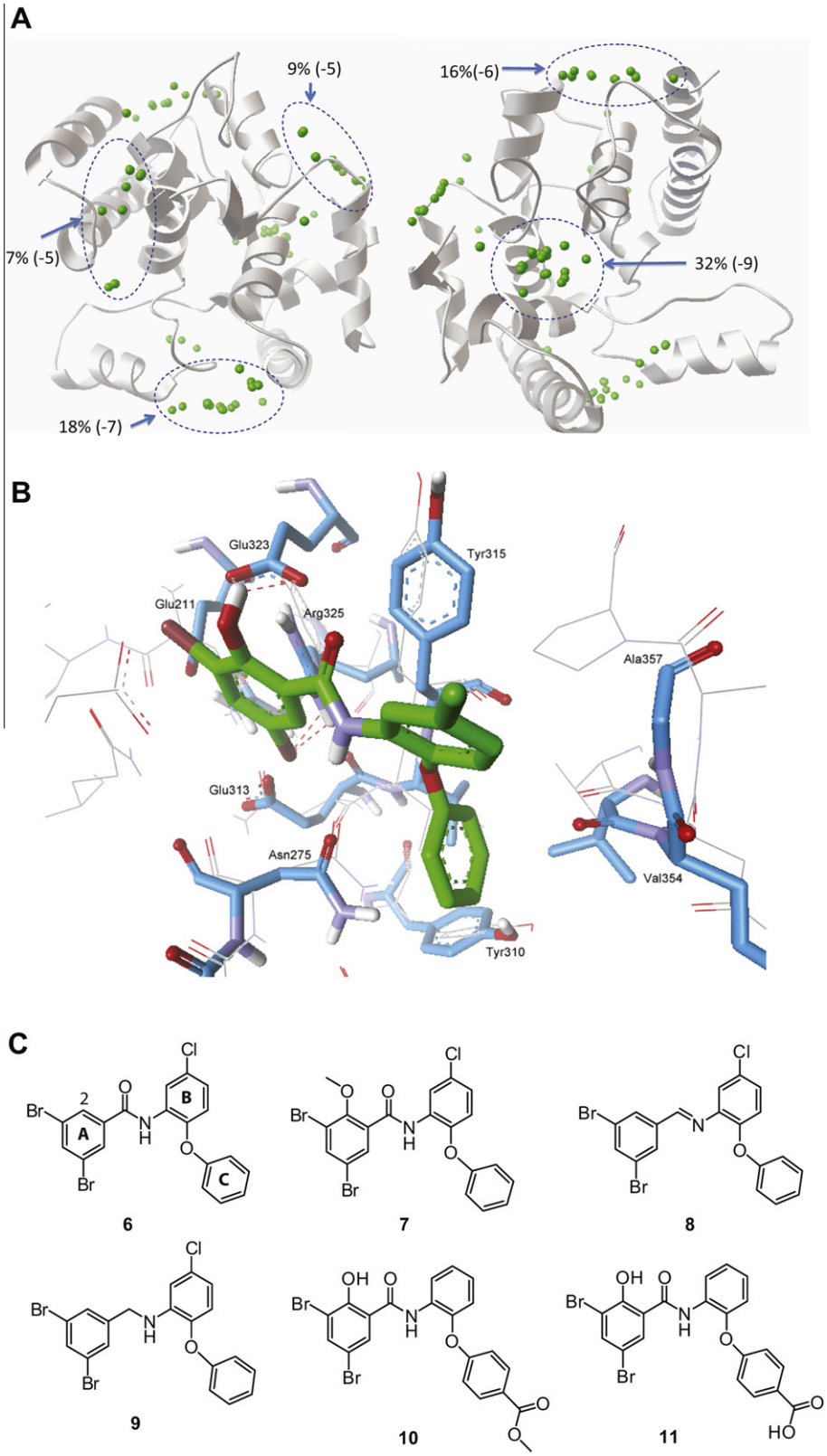

Figure 7. Modeling analysis of 42-10 (**2**) in complex with TGase. (A) Results of blind docking of compound **2** to the surface of the TGase (PDB code 3hzs). Compound **2** mostly (~32%; avg score = −9 kcal/mol) fell within the moenomycin binding site.[19,20] (B) The modeled complex of compound **2** with *E. coli* PBP (3fwl, blue stick presentation). The main residues for interaction, Asn275, Tyr310, Tyr315, Ile314, Glu323, Arg325, Val354, and Ala357 were labeled. Compound **2** was shown in green stick. The reference structure (PDB coded 3hzs) was shown in grey wire. Nitrogen is in blue, oxygen in red, bromine in dark red, and chlorine in green. (C) The structures of the compounds **6**–**11** prepared to identify the essential moieties in compound 42-10 (**2**). Except compound **10**, the other five compounds showed no TGase inhibition activities at 100 μM.

(NBD)-labeled lipid II and full-length PBP from EC, SA, and Mtb[18] in tubes containing 10 ng/μL *N*-acetylmuramidase in 50 mM Tris·HCl (pH 8.0), 10 mM $MgCl_2$, 0.1% Triton X-100, 10% DMSO, and 15% MeOH for 30 min. Reaction supernatants were then injected onto an anion-exchange HPLC column (SAX1, Supelco Co.) and eluted with a linear gradient of ammonium acetate (20 mM–0.5 M) in

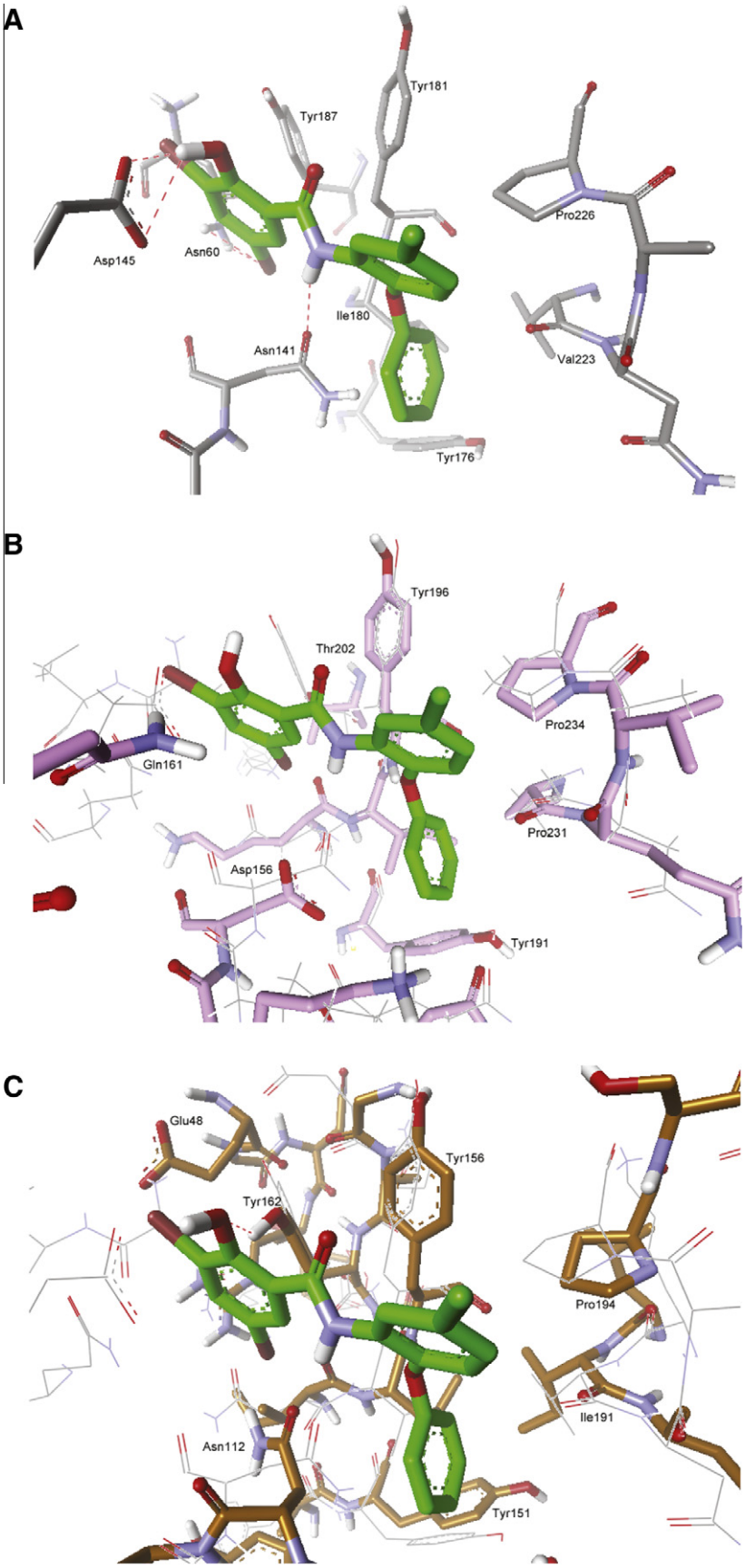

Figure 8. Modeling analysis of compound **2** in complex with (A) reference structure SA MtgA (PDB code 3hzs), (B) SA PBP (PDB code 2olv), and (C) Mtb *PonA* (homology modeling). Protein residues were illustrated in stick shape and colored in grey (A), in pink (B) or in brown (C). Compound **2** was shown in green stick. For comparison, the reference structure was also shown in grey wire. Nitrogen is in blue, oxygen in red, bromine in dark red, and chlorine in green.

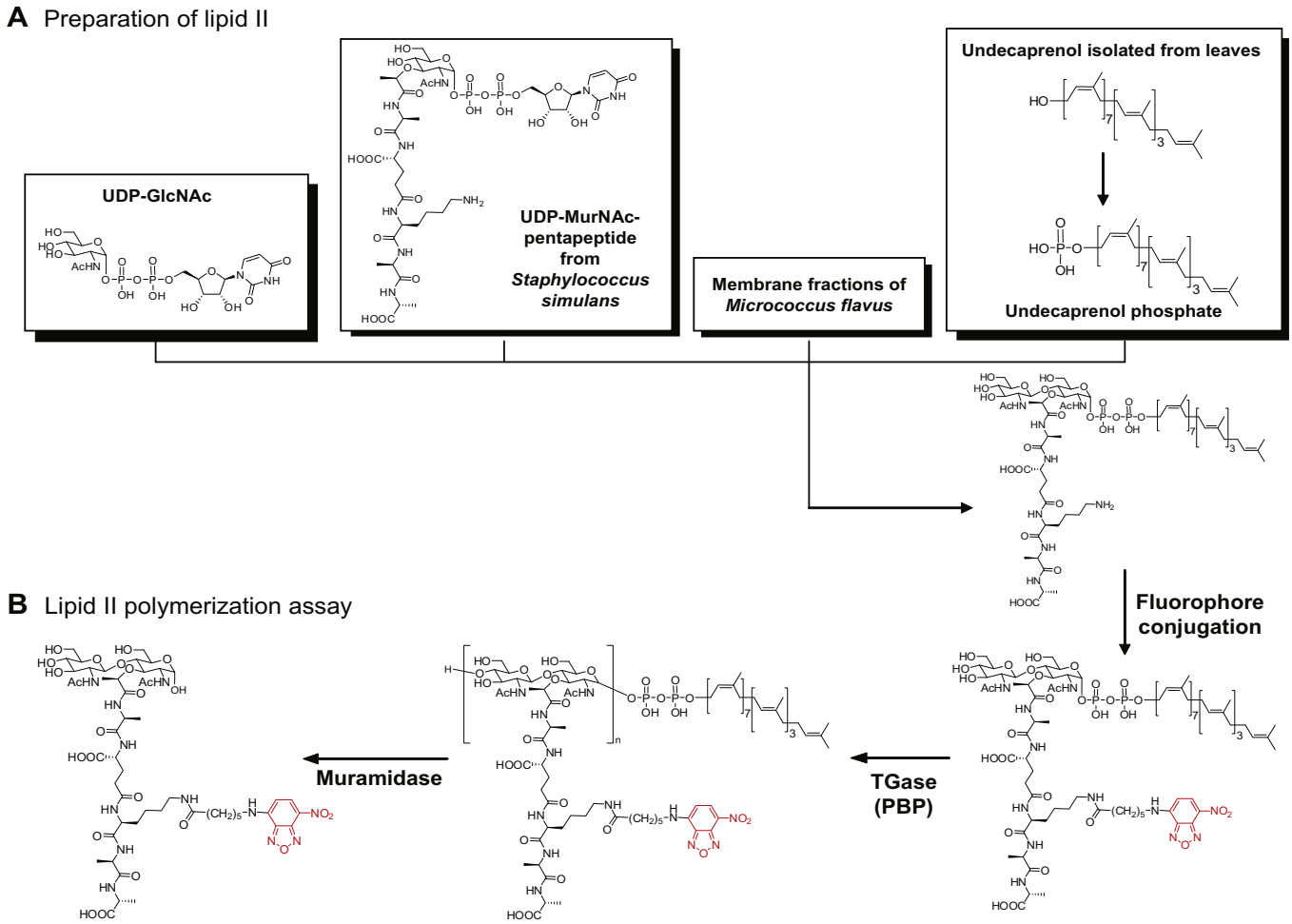

Figure 9. Preparation of lipid II (A) and lipid II polymerization assay (B). (A) Lipid II was prepared using chemoenzymatic method and conjugated with a fluorophore as described in the Section 4. (B) NBD (marked in red)-labeled lipid II was polymerized by functional TGase. The polymerized lipid II was further digested with muramidase and the digested peptidoglycan monomer was analyzed by HPLC chromatography.

methanol. The eluant was monitored for fluorescence with λ_{ex} = 466 nm and λ_{em} = 535 nm. The compound concentration that inhibits at least 90% of the reaction was defined as IC_{90} and used for activities comparison between the analogues.

4.8. Modeling analysis

Theoretical complexes of potent compounds with the target were obtained by a blind docking, which was introduced by scanning the entire surface of the target for a focused site, followed by a site-focused docking by using Autodock.[36] Autodock method was set to the Lamarckian Genetic Algorithm (LGA). The grid maps were defined using AutoGrid. For blind docking, the grid size was set to 120 × 120 × 120 points with a grid spacing of 0.185 Å centered on the mass center of the protein; for focused docking, the grid size was set to 60 × 60 × 60 points to cover the entire binding pocket. Step sizes of 1 Å for translation and 5° for rotation were chosen, a maximum number of energy evaluations was set to 1,500,000. For each independent runs, a maximum number of 270,000 LGA operations were generated on a single population of 100 individuals. Operator weights for crossover, mutation, and elitism were set to 0.80, 0.02, and 1, respectively.

The structures of SA monofunctional glycosyltransferase MtgA (PDB code 3hzs),[20] the EC bifunctional TGase (PDB code 3fwl)[19] and SA bifunctional TGase (PDB code 2olv)[21] were used for docking analysis. The molecular structure of Mtb PBP encoded by *ponA* gene was obtained from Protein Model Portal.[22] The homology modeling used both 2oqo (39% sequence identity) and 2olu (24% sequence identity) as templates. The obtained structure was refined with Impact® Energy Minimization module (Schrodinger Inc., USA) with OPLS_2005 force field. The resultant structure was then superimposed on molecular structure of SA glycosyltransferase MtgA (PDB code 3hzs) to obtain new atom coordinates for feature comparison structurally.

4.9. Salicylanilide analogues

Salicylanilide analogues 42-1–42-19 and 42-30–42-37 were obtained from ChemDiv (San Diego, CA, USA). Compounds 42-21–42-29 and 42-38–42-54 were obtained from ChemBridge (San Diego, CA, USA). All compounds were >90% pure. The purity was measured by analytical HPLC and the spectra were recorded at 260 nm. Preparation of compounds **6–11** was described in Supplementary data.

Acknowledgements

The authors thank the reviewers for valuable suggestions. This work was supported by the Summit program and Academia Sinica in Taiwan (to Dr. Chi-Huey Wong). The authors express their gratitude for this support.

A. Supplementary data

Supplementary data associated with this article can be found, in the online version, at doi:10.1016/j.bmc.2010.10.036.

References and notes

1. Silver, L. L. *Curr. Opin. Microbiol.* **2003**, *6*, 431.
2. Pedersen, L. C.; Benning, M. M.; Holden, H. M. *Biochemistry* **1995**, *34*, 13305.
3. Speer, B. S.; Shoemaker, N. B.; Salyers, A. A. *Clin. Microbiol. Rev.* **1992**, *5*, 387.
4. Bearden, D. T.; Danziger, L. H. *Pharmacotherapy* **2001**, *21*, 224S.
5. Kahne, D.; Leimkuhler, C.; Lu, W.; Walsh, C. *Chem. Rev.* **2005**, *105*, 425.
6. Bouhss, A.; Trunkfield, A. E.; Bugg, T. D.; Mengin-Lecreulx, D. *FEMS Microbiol. Rev.* **2008**, *32*, 208.
7. Liu, H.; Ritter, T. K.; Sadamoto, R.; Sears, P. S.; Wu, M.; Wong, C. H. *Chembiochem* **2003**, *4*, 603.
8. Sauvage, E.; Kerff, F.; Terrak, M.; Ayala, J. A.; Charlier, P. *FEMS Microbiol. Rev.* **2008**, *32*, 234.
9. Shahid, M.; Sobia, F.; Singh, A.; Malik, A.; Khan, H. M.; Jonas, D.; Hawkey, P. M. *Crit. Rev. Microbiol.* **2009**, *35*, 81.
10. Izat, A. L.; Colberg, M.; Reiber, M. A.; Adams, M. H.; Skinner, J. T.; Cabel, M. C.; Stilborn, H. L.; Waldroup, P. W. *Poult. Sci.* **1990**, *69*, 1787.
11. Wallhausser, K. H.; Nesemann, G.; Prave, P.; Steigler, A. *Antimicrob. Agents Chemother. (Bethesda)* **1965**, *5*, 734.
12. Dealy, J.; Moeller, M. W. *J. Anim. Sci.* **1976**, *42*, 1331.
13. Dealy, J.; Moeller, M. W. *J. Anim. Sci.* **1977**, *45*, 1239.
14. Liu, H.; Wong, C. H. *Bioorg. Med. Chem.* **2006**, *14*, 7187.
15. Ostash, B.; Doud, E. H.; Lin, C.; Ostash, I.; Perlstein, D. L.; Fuse, S.; Wolpert, M.; Kahne, D.; Walker, S. *Biochemistry* **2009**, *48*, 8830.
16. Shih, H. W.; Chen, K. T.; Chen, S. K.; Huang, C. Y.; Cheng, T. J.; Ma, C.; Wong, C. H.; Cheng, W. C. *Org. Biomol. Chem.* **2010**, *8*, 2586.
17. Zhang, J. H.; Chung, T. D.; Oldenburg, K. R. *J. Biomol. Screen.* **1999**, *4*, 67.
18. Cheng, T. J.; Sung, M. T.; Liao, H. Y.; Chang, Y. F.; Chen, C. W.; Huang, C. Y.; Chou, L. Y.; Wu, Y. D.; Chen, Y. H.; Cheng, Y. S.; Wong, C. H.; Ma, C.; Cheng, W. C. *Proc. Natl. Acad. Sci. U.S.A.* **2008**, *105*, 431.
19. Sung, M. T.; Lai, Y. T.; Huang, C. Y.; Chou, L. Y.; Shih, H. W.; Cheng, W. C.; Wong, C. H.; Ma, C. *Proc. Natl. Acad. Sci. U.S.A.* **2009**, *106*, 8824.
20. Heaslet, H.; Shaw, B.; Mistry, A.; Miller, A. A. *J. Struct. Biol.* **2009**, *167*, 129.
21. Lovering, A. L.; de Castro, L. H.; Lim, D.; Strynadka, N. C. *Science* **2007**, *315*, 1402.
22. Arnold, K.; Kiefer, F.; Kopp, J.; Battey, J. N.; Podvinec, M.; Westbrook, J. D.; Berman, H. M.; Bordoli, L.; Schwede, T. *J. Struct. Funct. Genomics* **2009**, *10*, 1.
23. De La Fuente, R.; Sonawane, N. D.; Arumainayagam, D.; Verkman, A. S. *Br. J. Pharmacol.* **2006**, *149*, 551.
24. Ferriz, J. M.; Vavrova, K.; Kunc, F.; Imramovsky, A.; Stolarikova, J.; Vavrikova, E.; Vinsova, J. *Bioorg. Med. Chem.* **2010**, *18*, 1054.
25. Boyce, J. P.; Brown, M. E.; Chin, W.; Fitzner, J. N.; Paxton, R. J.; Shen, M.; Stevens, T.; Wolfson, M. F.; Wright, C. D. *Bioconjugate Chem.* **2008**, *19*, 1775.
26. Liechti, C.; Sequin, U.; Bold, G.; Furet, P.; Meyer, T.; Traxler, P. *Eur. J. Med. Chem.* **2004**, *39*, 11.
27. Imramovsky, A.; Vinsova, J.; Ferriz, J. M.; Dolezal, R.; Jampilek, J.; Kaustova, J.; Kunc, F. *Bioorg. Med. Chem.* **2009**, *17*, 3572.
28. Macielag, M. J.; Demers, J. P.; Fraga-Spano, S. A.; Hlasta, D. J.; Johnson, S. G.; Kanojia, R. M.; Russell, R. K.; Sui, Z.; Weidner-Wells, M. A.; Werblood, H.; Foleno, B. D.; Goldschmidt, R. M.; Loeloff, M. J.; Webb, G. C.; Barrett, J. F. *J. Med. Chem.* **1998**, *41*, 2939.
29. Welzel, P. *Angew. Chem., Int. Ed.* **2007**, *46*, 4825.
30. Taylor, J. G.; Li, X.; Oberthur, M.; Zhu, W.; Kahne, D. E. *J. Am. Chem. Soc.* **2006**, *128*, 15084.
31. Trepalin, S. V.; Gerasimenko, V. A.; Kozyukov, A. V.; Savchuk, N. P.; Ivaschenko, A. A. *J. Chem. Inf. Comput. Sci.* **2002**, *42*, 249.
32. Willett, P. *Curr. Opin. Biotechnol.* **2000**, *11*, 85.
33. Nikolovska-Coleska, Z.; Wang, R.; Fang, X.; Pan, H.; Tomita, Y.; Li, P.; Roller, P. P.; Krajewski, K.; Saito, N. G.; Stuckey, J. A.; Wang, S. *Anal. Biochem.* **2004**, *332*, 261.
34. Breukink, E.; van Heusden, H. E.; Vollmerhaus, P. J.; Swiezewska, E.; Brunner, L.; Walker, S.; Heck, A. J.; de Kruijff, B. *J. Biol. Chem.* **2003**, *278*, 19898.
35. VanNieuwenhze, M. S.; Mauldin, S. C.; Zia-Ebrahimi, M.; Winger, B. E.; Hornback, W. J.; Saha, S. L.; Aikins, J. A.; Blaszczak, L. C. *J. Am. Chem. Soc.* **2002**, *124*, 3656.
36. Goodsell, D. S.; Morris, G. M.; Olson, A. J. *J. Mol. Recognit.* **1996**, *9*, 1.